Metals and Materials International (2021) 27:3959–3967
https://doi.org/10.1007/s12540-021-00968-x

# Influence of Microstructure Constituents on the Hydrogen-Induced Mechanical Degradation in Ultra-High Strength Sheet Steels

A In Hwang[1] · Dae Geon Lee[1] · Yeonseung Jung[2] · Jin-Mo Koo[2] · Jae Dong Cho[2] · Jae Sang Lee[1] · Dong-Woo Suh[1]

Received: 20 December 2020 / Accepted: 4 January 2021 / Published online: 12 May 2021


**Abstract**
We investigate the influence of constituent phases on the hydrogen-induced mechanical degradation in two ultra-high strength sheet steels. In the complex phase (CP) steel, of which microstructure can be regarded as monolithic in terms of hydrogen behaviors, the rate of hydrogen uptake gradually decreases with the charging time, while the transformation-induced plasticity (TRIP) steel exhibits a persistent hydrogen absorption up to the charging time of 48 h, which is attributed to the presence of austenite. The mechanical degradation of TRIP steel goes beyond that of the CP steel at charging time over 12 h, coincident with the condition in which the austenite contributes to the hydrogen uptake. Both the ultra-high strength and the presence of austenite have unfavorable influence on the hydrogen embrittlement. Therefore, in the TRIP steel, it is necessary to evaluate quantitatively the critical hydrogen concentration over which more care should be taken to reduce the risk of hydrogen-induced mechanical degradation.

**Keywords** Ultra-high strength · Steels · Hydrogen · Microstructure · Austenite

## 1 Introduction

Very small amount of hydrogen in steel can deteriorate the mechanical performance significantly. It is called as hydrogen embrittlement and has been one of the important issues, particularly, in the wire and rod steel products [1, 2]. Tensile strengths of those steels often exceed 1 GPa that is a critical value to consider a risk of the mechanical degradation by hydrogen [3–6]. Recently, concern on hydrogen embrittlement is growing in the sheet steels for automotive parts [7, 8]; it is attributed to the increased strength level keeping pace with the safety requirement as well as the weight reduction of body-in-white [9]. For instance, ultra-high strength steels having tensile strength over 1.2 GPa are actively applied to secure the crush worthiness.

Dissimilar to the wire and rod products, the sheet steels usually contain multiphase microstructure to obtain the strength-elongation balance [10–12]. Typical constituent phases utilized in ultra-high strength sheet steels are bainite, martensite and retained austenite [13]. In certain cases, ferrite is also employed to achieve desired ductility. Since the characteristics of constituent phases heavily affect the hydrogen uptake and diffusion behavior, which are critical parameters in the hydrogen embrittlement susceptibility, the multiphase microstructures of ultra-high strength sheet steels make the hydrogen-induced mechanical degradation more complicated phenomena [14–16].

Various microstructure concepts have been proposed in the sheet steels and succeeded in obtaining ultra-high strength without serious loss of elongation [17–19]. Nevertheless, the influence of microstructure constituents on the hydrogen uptake and diffusion behaviors in ultra-high strength multiphase steels are not sufficiently investigated so far. Given that the reliability of mechanical performance is one of the essential indices for the application of ultra-high strength sheet steels to the structural parts, a quantitative analysis on the hydrogen behaviors depending on the constituent phases is crucial regarding not only to the scientific aspect but also to the industrial perspective. Therefore, in the present study, we conducted a comprehensive

✉ Dong-Woo Suh
dongwoo1@postech.ac.kr

[1] Graduate Institute of Ferrous & Energy Materials Technology (GIFT), POSTECH, Pohang 37673, Republic of Korea

[2] Technical Research Laboratories, POSCO, Pohang 37859, Republic of Korea

study on the hydrogen behaviors and resultant mechanical degradations in two representative ultra-high strength sheet steels: complex phase (CP) steel and transformation-induced plasticity (TRIP) steel. We aim to examine the hydrogen uptake and diffusion in dissimilar microstructure of ultra-high strength sheet steels, and to investigate the corresponding mechanical response associated with the hydrogen behavior; thereby it is expected to provide an insight for the microstructure design in ultra-high strength sheet steels compromising the mechanical performance and the reliability related to the hydrogen.

## 2 Experimental procedures

Table 1 shows the chemical compositions of investigated steels. The complex phase (CP) steel and transformation-induced plasticity (TRIP) steel is designated as CP and TRIP, respectively. They are ultra-high strength steels with tensile strength over 1180 MPa. The steel sheets are delivered as cold-rolled and heat-treated condition with a thickness approximately 1 mm. Microstructure of the steels were observed using a scanning electron microscope (SEM) with electron back scattered diffraction (EBSD). For the SEM and EBSD analysis, electrochemical polishing was conducted in a solution of 5% $HClO_4$ + 95% $CH_3COOH$. The retained austenite fraction was quantified using integrating intensity of $(111)_\gamma$, $(200)_\gamma$, $(220)_\gamma$, $(311)_\gamma$ and $(110)_\alpha$, $(200)_\alpha$, $(211)_\alpha$, $(220)_\alpha$ peaks obtained from the XRD [20, 21]. Hydrogen charging was carried out electrochemically using a pair of subsized tensile specimens (ASTM E8M) in an aqueous solution of 3% NaCl containing 3 g/l $NH_4SCN$ with a current density of 1 A/m$^2$ for 1–48 h at room temperature. Amount of diffusible hydrogen content was measured using a quadruple mass spectroscope (Q-mass) at a heating rate of 100 °C/h to 300 °C. Mechanical degradation at presence of hydrogen was evaluated by a slow strain tensile test (SSRT) at a strain rate of $10^{-5}$ /s. To prevent hydrogen effusion during the SSRT, Zn plating was conducted on the tensile specimen after the hydrogen charging. Effective diffusivity and apparent solubility of hydrogen was estimated by a hydrogen permeation test complying to ISO 17,081 [22]. Time lag method, $D_{eff} = L^2 / 6t_l$, was used, where L is specimen thickness and $t_l$ is time lag defined to be that required to achieve 0.63 of the steady-state current density on the permeation curve.

## 3 Results and discussion

### 3.1 Microstructure and hydrogen uptake

Microstructure of the CP steel consists of bainite and martensite with ferrite (Fig. 1a), while the major microstructure constituents in TRIP steel are bainitic ferrite and retained austenite (Fig. 1c). The EBSD phase maps in Figs. 1b and d reveal that austenite fraction in the CP steel is negligible but the presence of fine austenite grains in the TRIP steel with the size around 0.5 μm (Fig. 1d). The austenite fraction is evaluated to be nearly 0% and 15% in the CP and TRIP steel, respectively, using the XRD profiles in Fig. 2. Representative stress–strain curves using SSRT indicate that the tensile strength of both steels are over 1180 MPa (Fig. 3). It is noted that the tensile strength and total elongation of TRIP steel is rather higher than those of CP steel, which is presumably coming from the enhanced work hardening by deformation-induced transformation of austenite into martensite [23, 24]. The gradual decrease of austenite fraction with tensile elongation (Fig. 4, black symbols) confirms the formation of martensite in the course of deformation.

Figure 5a, b are hydrogen desorption curves after electrochemical charging for given times. Most of hydrogen is released below 200 °C, indicating the major trapping sites of hydrogen are reversible ones in both steels [25–27]. The amount of diffusible hydrogen in the CP steel (Fig. 6a) is gradually increased with the charging time; while the rate of hydrogen uptake become slow as the charging time increases, indicating a saturation of hydrogen absorption at the prolonged charging time. On the other hand, the hydrogen uptake in the TRIP steel exhibits rather different feature (Fig. 6b). The amount of hydrogen in the TRIP steel increases with the charging time; however, a transition in the charging behavior is observed around the charging time between 8–12 h and the amount of hydrogen keep increasing at the prolonged charging time. It suggests that the hydrogen uptake continuously proceeds without saturation for given charging conditions. Different hydrogen absorption behavior in the CP and TRIP steels is thought to be related to the dissimilar microstructure constituent in both steels. As mentioned, the microstructure of the CP steel is composed of bainite, martensite and ferrite. Even though the strength levels of those phases are quite diverse, the diffusivity and solubility of hydrogen in those phases are comparable because they have nearly the same crystal structure (BCC or BCT close to BCC). Meanwhile, the TRIP steel contains considerable amount of retained austenite (~ 15%) having a crystal structure of FCC. The behavior of hydrogen in austenite is significantly different from that in remaining microstructure constituent such as bainitic ferrite. For instance, the diffusivity of hydrogen is orders of magnitude slow in austenite compared to that in ferrite [28], while the solubility of hydrogen far larger in austenite than that in

**Table 1** Chemical composition of investigated steels (wt%)

| | C | Mn | Si | Others |
|---|---|---|---|---|
| CP | 0.12 | 2.3 | 1.0 | < 1.0 |
| TRIP | 0.17 | 2.6 | 1.5 | < 0.3 |

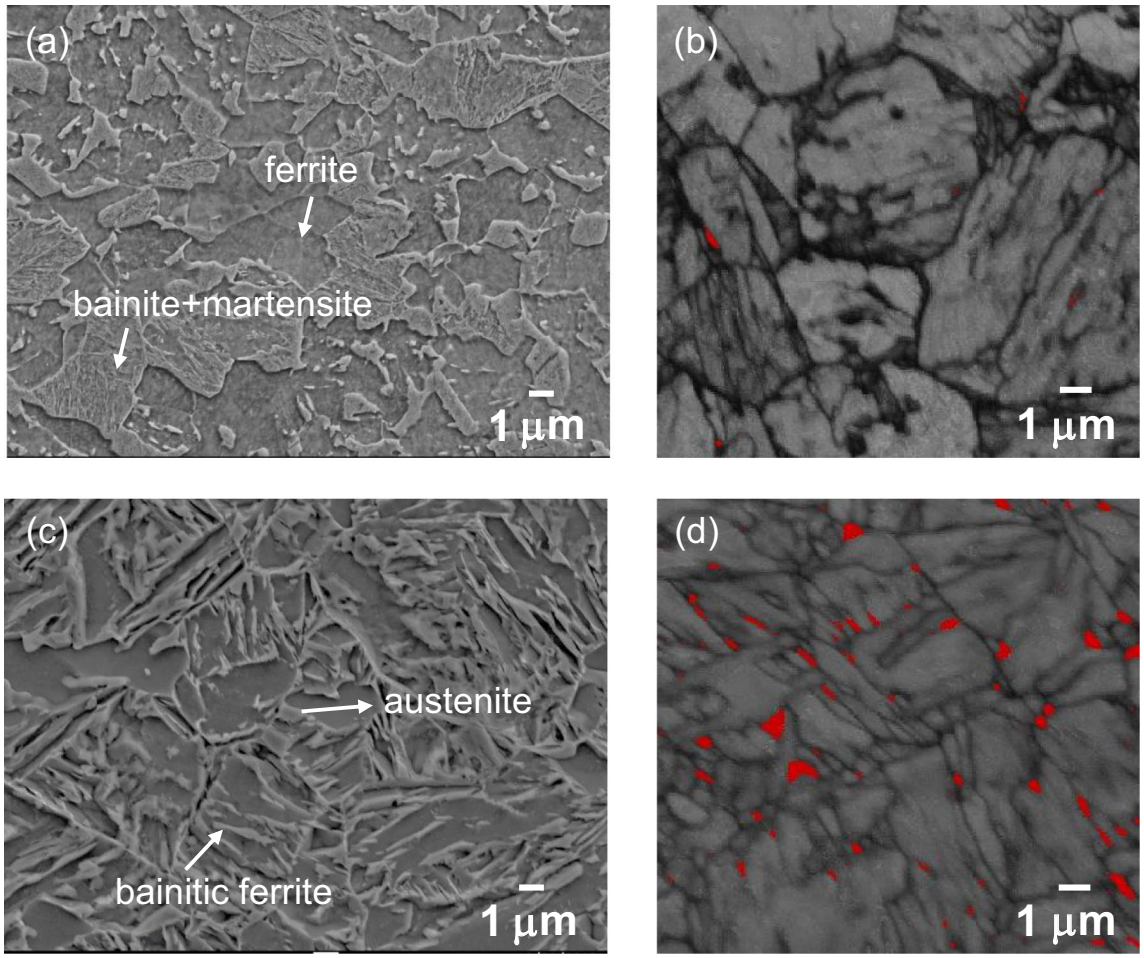


**Fig. 1** SEM micrographs of **a** CP steel and **c** TRIP steel and EBSD phase maps of **b** CP steel and **d** TRIP steel (Red regions in the phase maps represent the FCC phase and the average confidence index was above 0.65. The step size was 40 nm for EBSD measurement)

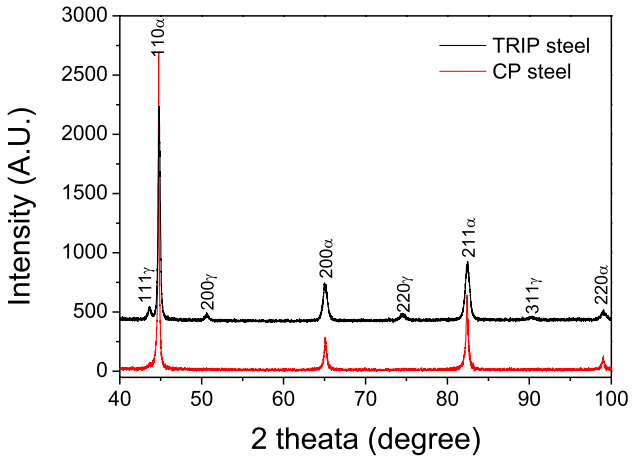


**Fig. 2** XRD profiles of the investigated steels

ferrite [29–31]. Given that the austenite grains are isolated by continuous matrix of bainitic ferrite in the TRIP steel (Fig. 1d), it is reasonable to presume that the hydrogen permeates the bainitic ferrite preferentially, and uptake into the austenite occurs subsequently [32]. In that sense, the rapid increase of hydrogen content in earlier charging time up to 12 h is mainly led by the absorption of hydrogen by bainitic ferrite but the further increase of hydrogen content at the prolonged charging time is also attributed to the hydrogen uptake into austenite. Persistent increase of hydrogen content in the charging time over 12 h in the TRIP steel, which is different from the gradual saturation of hydrogen content observed in the CP steel, is consistent with the larger hydrogen solubility in austenite. Table 2 shows the effective diffusivity and apparent solubility of hydrogen evaluated from the permeation curves (Fig. 7). The TRIP steels exhibits lower diffusivity but larger solubility of hydrogen compared

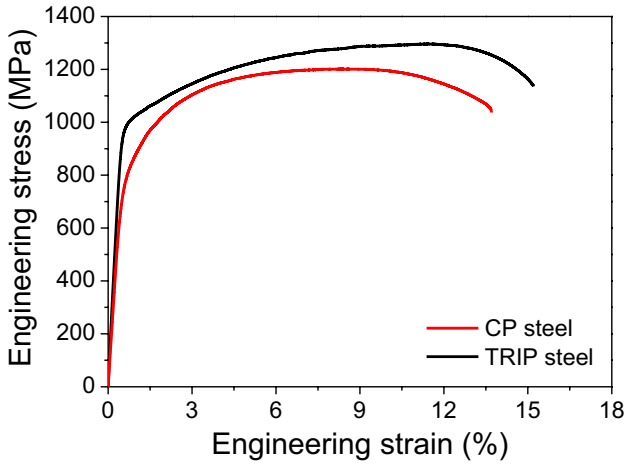


**Fig. 3** Stress–strain curves of the investigated steels subjected to slow strain tensile tests (without hydrogen charging)

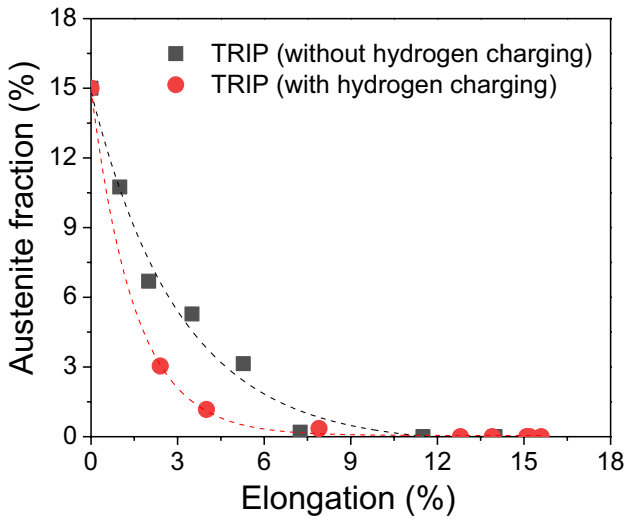


**Fig. 4** Change of austenite fraction with respect to the tensile deformation (black symbols: hydrogen-free, red symbols: hydrogen-charged condition)

to those in CP steel; it suggests that the TRIP steel absorbs more hydrogen due to the presence of retained austenite even though the rate of hydrogen uptake into austenite is slow. It accords with the nearly constant increase of hydrogen content at the prolonged charging time up to 48 h in the TRIP steel (Fig. 6b).

### 3.2 Influence of constituent phase on hydrogen-induced mechanical degradation

The stress–strain curves of CP and TRIP steels subjected to the hydrogen charging show degradations in elongation as well as tensile strength (Fig. 8). The tensile properties of both steels are deteriorated as the charging time increases; nevertheless, it is noted that the susceptibility to the hydrogen-induced mechanical degradation appears to be different in both steels at longer charging time (Fig. 9). When the hydrogen charging time is shorter than 12 h, mechanical degradation in both steels is comparable. However, the elongation loss in the TRIP steel goes beyond that in the CP steel at charging time longer than 12 h and ends up with approximately 20% higher value at charging time of 48 h. When it comes to the loss in tensile strength, the difference between the CP and TRIP steels becomes more obvious. The loss in tensile strength is less than 5% for all charging conditions in the CP steel but that of the TRIP steel increases remarkably after hydrogen charging of 12 h, and reaches to around 20% at the charging time of 48 h.

The hydrogen uptake behaviors (Fig. 6) and corresponding mechanical degradations (Fig. 9) gives a clue to understand the different hydrogen susceptibility in both steels. As mentioned, the hydrogen uptake during electrochemical charging is affected by the characteristics of microstructure constituent of the CP and TRIP steels. Given that the CP steel has a monolithic microstructure in terms of the hydrogen behavior, the TRIP steel contains retained austenite having slower diffusivity and larger solubility of hydrogen compared bainitic ferrite matrix; it is thought to lead to the nearly constant increase of hydrogen content after the charging time of 12 h (Fig. 6b). Then the coincidence of the charging time, at which the retained austenite actively contributes to the hydrogen uptake and the significant deterioration of elongation and tensile strength in the TRIP steel happens, implies that the hydrogen absorption into the retained austenite plays a role in the pronounced mechanical degradation in the TRIP steel.

Even though the diffusion of hydrogen in austenite is very slow compared to that in bainitic ferrite, larger amount of hydrogen can be dissolved in austenite; therefore, once the austenite is enriched with hydrogen and subsequently exposed to the deformation, the stress- or strain-induced martensitic transformation is likely to generate hydrogen-supersaturated fresh martensite. It has been reported that the fresh martensite is vulnerable microstructure to the occurrence of hydrogen embrittlement [33, 34]. Besides, since supersaturated hydrogen in martensite has higher diffusivity than that in austenite, it can migrate into various types of adjacent interfaces in a short time, leading to the deterioration of ductility [32]. Actually, the austenite fraction measured in the hydrogen charged specimens fractured at corresponding tensile elongations (Fig. 4, red symbols) clearly indicates that significant amount of retained austenite transformed into martensite upon deformation, which implies the generation of hydrogen-enriched fresh martensite. Overlapping of the change of austenite fraction with respect to the tensile elongation in hydrogen-free and hydrogen charged

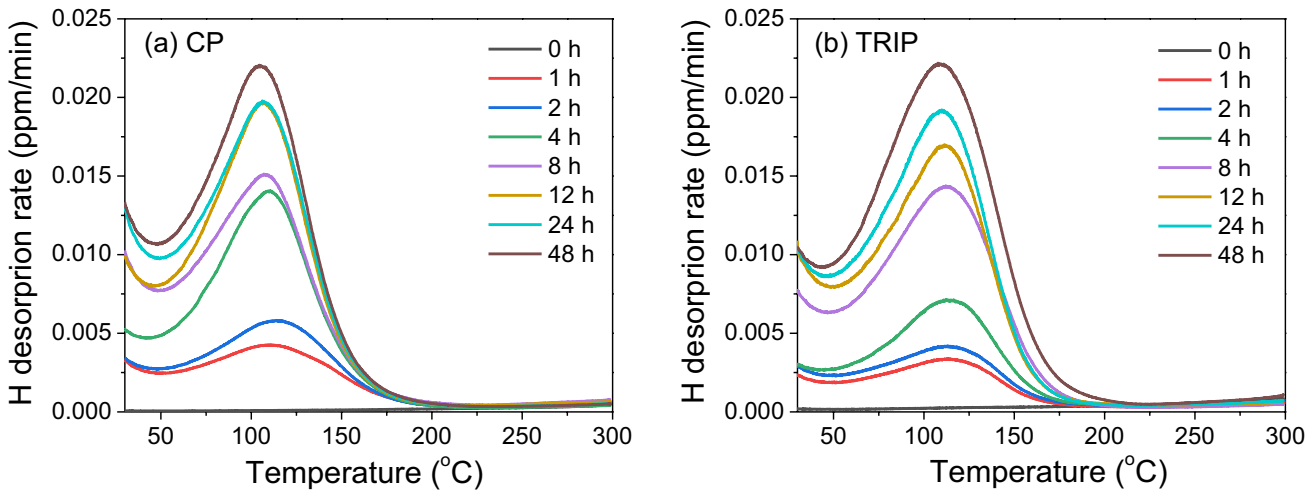


**Fig. 5** Hydrogen desorption curves with charging time **a** CP steel and **b** TRIP steel

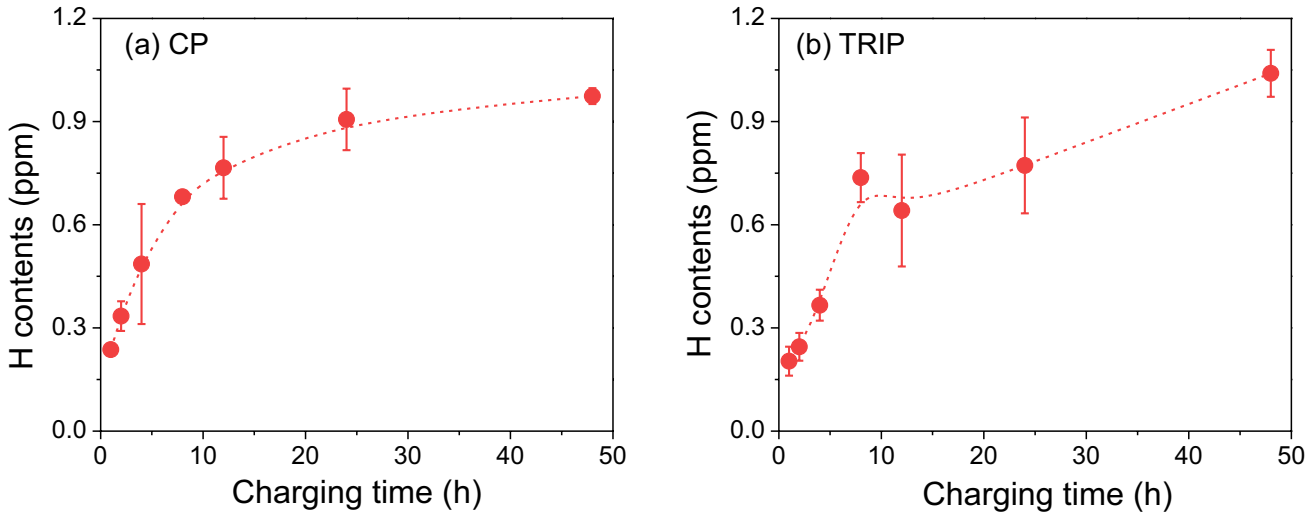


**Fig. 6** Hydrogen content with charging time **a** CP steel and **b** TRIP steel

specimen in Fig. 4, it seems that the presence of hydrogen in austenite deteriorates the mechanical stability of austenite [35]. However, it has been a controversial issue [36] that needs a further investigation.

Figure 10 shows the fracture surfaces of the CP and TRIP steels after the SSRT. Without hydrogen, both steels exhibit ductile fracture surface covered with many dimples (Fig. 10a, d). As the charging time elapses, the depths of dimples become shallow and regions of brittle fracture surface (indicated with arrows) increases (Fig. 10b, e). At charging time of 24 h, brittle fracture surface prevails in both steels (Fig. 10c, f), yet more micro-cracks are found in the TRIP steel (indicated by arrows); it is in accordance with the severe mechanical degradation of the TRIP steel at the prolonged charging time. Given that higher population of micro-cracks in the TRIP steel at the charging time allowing hydrogen uptake into austenite, the hydrogen, originally enriched in austenite, can migrate in a short time into neighboring interfaces during the deformation-induced martensite transformation and increases a propensity to initiate cracks upon deformation, resulting in higher susceptibility to the hydrogen embrittlement.

It is worth mentioning that the loss of tensile strength in the TRIP steel becomes considerable with hydrogen charging over 12 h but it is nearly insensitive to the charging condition in the CP steel. It is because the work hardening of TRIP steel is primarily governed by the formation of deformation-induced martensite [24, 37, 38]. As mentioned, the deformation-induced martensite transformation from the hydrogen-enriched austenite enhances the propensity to

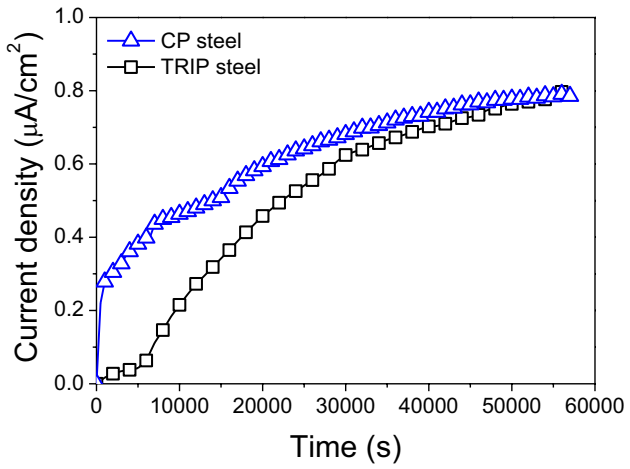


**Fig. 7** Hydrogen permeation curves of the investigated steels

**Table 2** Diffusion parameters evaluated using permeation tests

| | Effective diffusivity ($m^2/s$) | Apparent solubility ($mol/m^3$) |
|---|---|---|
| CP | $4.7 \times 10^{-11}$ | 3.5 |
| TRIP | $1.4 \times 10^{-11}$ | 8.0 |

List of figure caption

crack initiation in the neighboring interfaces. Therefore, the TRIP steel is prone to a premature fracture with hydrogen uptake, leaving some untransformed austenite grains that cannot contribute to the work hardening. In that circumstance, the TRIP steel cannot make full use of retained austenite to achieve the tensile strength without hydrogen. On the contrary, the work hardening of the CP steel is mainly involved with the dislocation interactions, which is less affected by the presence of hydrogen.

Finally, we would like to mention the susceptibility to the hydrogen embrittlement of the ultra-high strength sheet steels in the present study. Figure 11 summarizes the degradation of mechanical properties of the ultra-high strength CP and TRIP steels as a function of hydrogen contents. For comparison, the loss of elongation and tensile strength of TRIP 780 grade (tensile strength of 780 MPa) steel [34] and martensitic steel (4340 steel with tensile strength of 1500 MPa) [2] are also indicated. Note that the retained austenite fraction of TRIP 780 grade steel is 14.8% that is similar to that of the present TRIP steel (15%). Even with large difference in the tensile strength, the CP steel of the present study exhibits hydrogen-induced mechanical degradations comparable to that of TRIP 780 grade steel. Meanwhile, the ultra-high strength TRIP steel appears to be more sensitive to the hydrogen embrittlement than TRIP780 grade steel; losses of elongation and tensile strength at hydrogen content around 0.6 ppm in the ultra-high strength TRIP steel is similar to those at 1.2 ppm in the TRIP780 grade steel. It represents that both ultra-high tensile strength (over 1200 MPa) and presence of retained austenite have unfavorable influence on the hydrogen embrittlement. Nevertheless, the mechanical degradation of the present TRIP steel is comparable to that of the CP steel as long as the hydrogen content is less than approximately 0.6 ppm where the martensitic steel still experiences severe degradations in elongation and tensile strength. It suggests that the evaluation of critical hydrogen content, over which the risk of hydrogen-induced mechanical degradation sharply increases, is important to ensure the reliability of

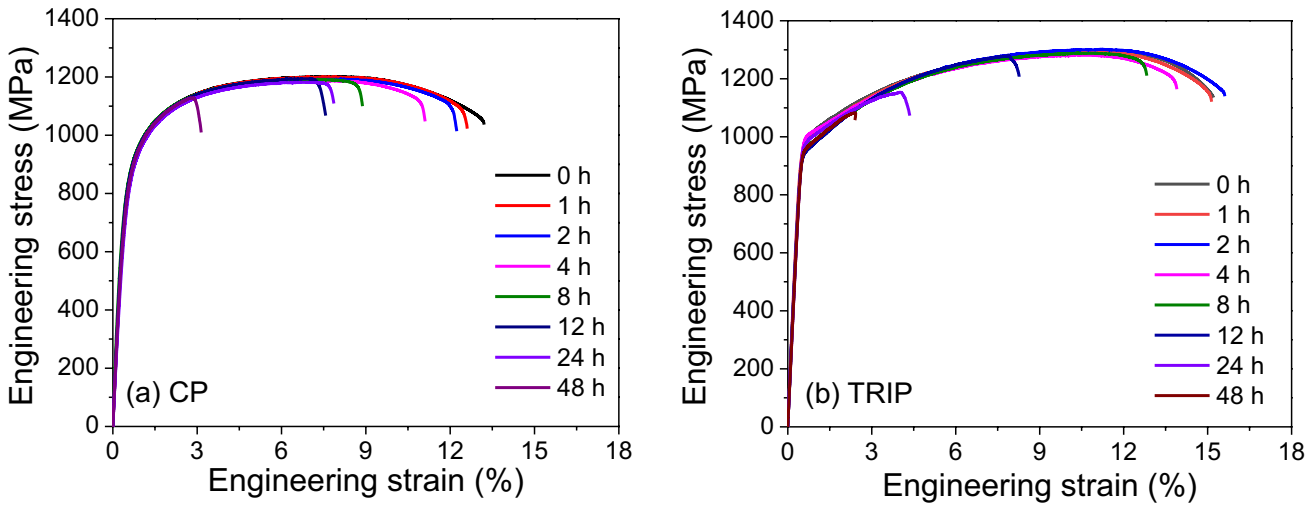


**Fig. 8** Stress–strain curves of **a** CP steel and **b** TRIP steel subjected to slow strain tensile tests (after hydrogen charging)

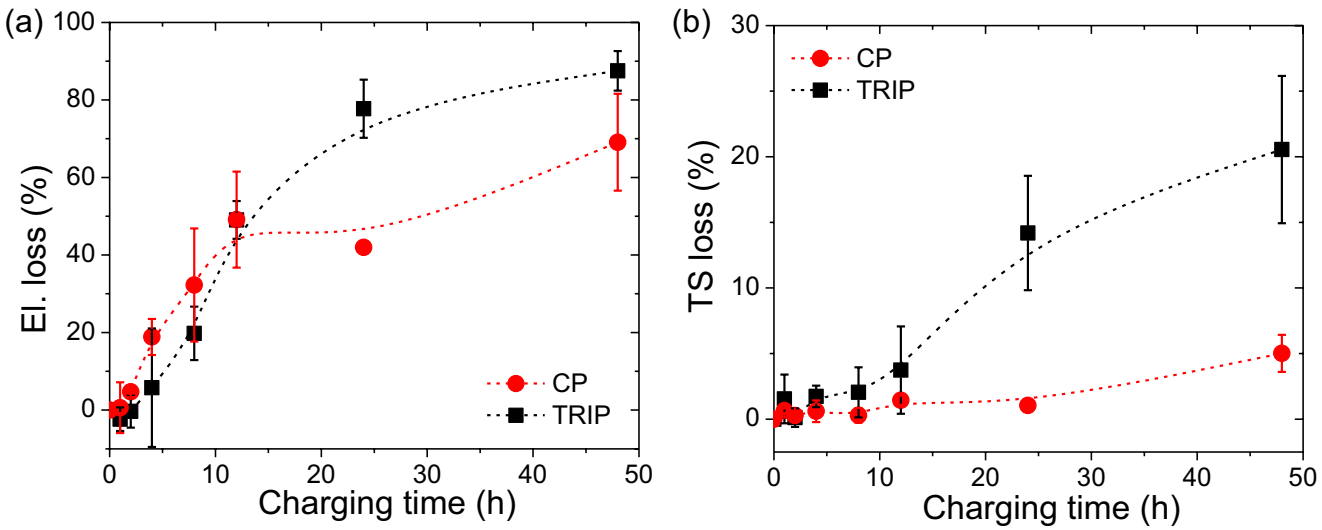


**Fig. 9** Loss of **a** elongation and **b** tensile strength with hydrogen charging in CP steel and TRIP steel

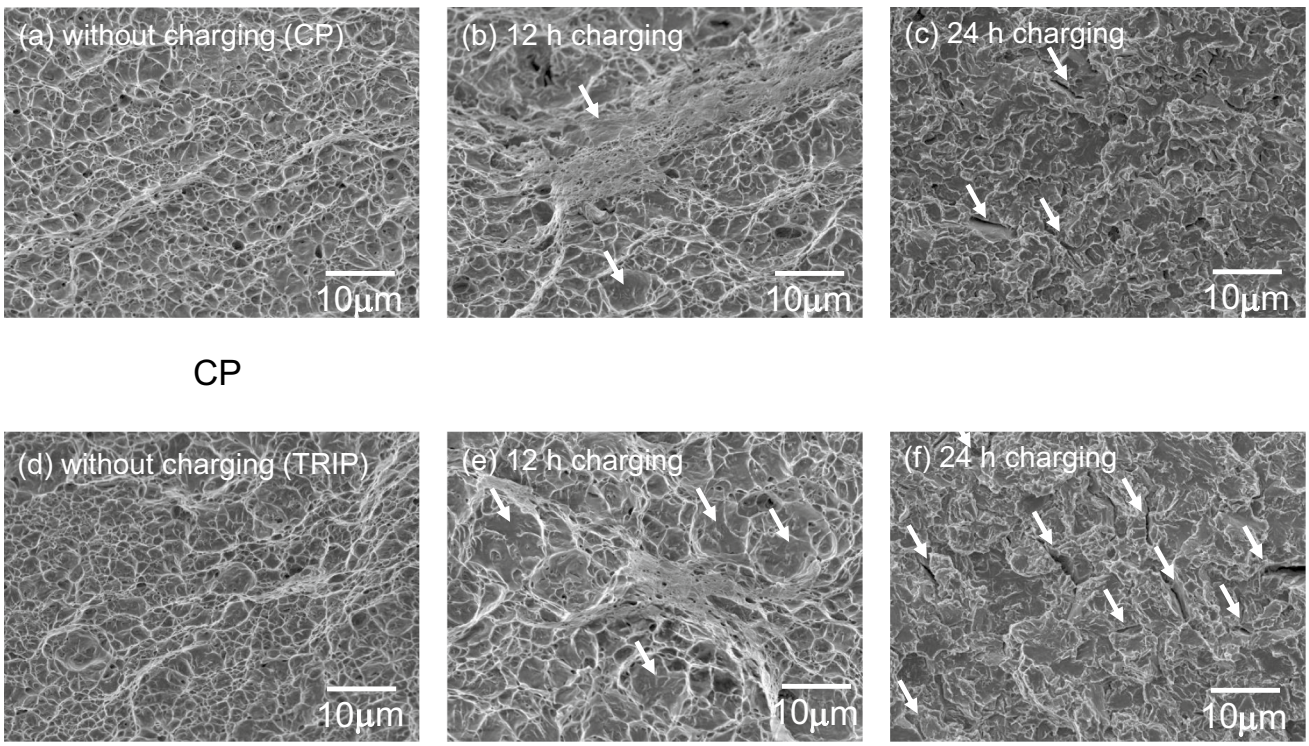


**Fig. 10** Fracture surfaces of (**a**–**c**) CP steel and (**d**–**f**) TRIP steels subjected to slow strain tensile tests

ultra-high strength TRIP steels at presence of hydrogen. Since the level of crucial hydrogen content is likely to be affected by microstructural features such as morphology of austenite [14], a proper microstructure control is desired to reduce the risk of hydrogen-induced mechanical degradation in ultra-high strength steel containing retained austenite.

## 4 Conclusions

Influence of microstructure constituent on the hydrogen-induced mechanical degradation is investigated in ultra-high strength CP and TRIP steels. Following conclusions can be drawn.

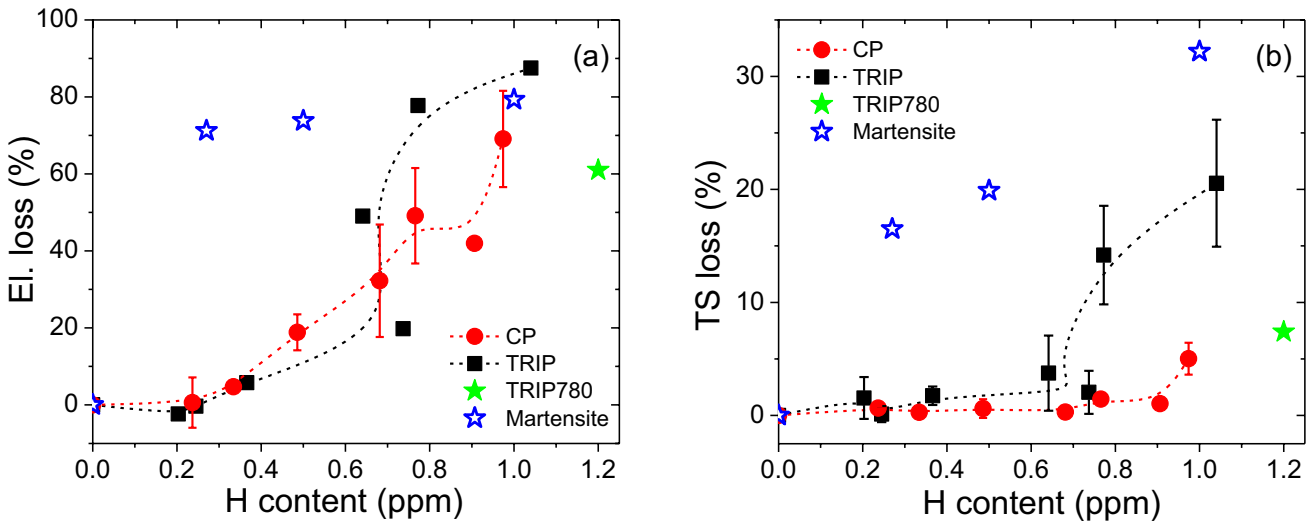


**Fig. 11** Loss of **a** elongation and **b** tensile strength with respect to the hydrogen content. Those of TRIP780 [34] and martensitic steels [2] are also presented

1. In the CP steel, the rate of hydrogen uptake gradually decreases with charging time. However, a transition in the charging behavior is observed at the charging time between 8–12 h and the rate of hydrogen uptake is nearly constant even with prolonged charging time up to 48 h in the TRIP steel.
2. Due to the presence of retained austenite, the TRIP steel exhibits slower effective diffusivity but larger apparent solubility of hydrogen than the CP steel. It leads to the persistent absorption of hydrogen in the TRIP steel at prolonged charging time.
3. The hydrogen-induced mechanical degradation in both steels are comparable up to the charging time of 12 h but the losses of elongation and tensile strength of the TRIP steel goes beyond those of the CP steel at the charging time longer than 12 h.
4. Ultra-high strength and presence of retained austenite in the TRIP steel have unfavorable influence regarding to the hydrogen embrittlement. It requires a sophisticated evaluation of critical hydrogen concentration over which more care should be taken to minimize the risk of hydrogen-induced mechanical degradation.

## References


1. G. Lovicu, M. Bottazzi, F. D'aiuto, M. De Sanctis, A. Dimatteo, C. Santus, R. Valentini, Metall. Mater. Trans. A **43**, 4075 (2012)
2. M. Wang, E. Akiyama, K. Tsuzaki, Corros. Sci. **49**, 4081 (2007)
3. H.K.D.H. Bhadeshia, ISIJ Int. **56**, 24 (2016)
4. I.M. Robertson, P. Sofronis, A. Nagao, M. Martin, S. Wang, D. Gross, K. Nygren, Metall. Mater. Trans. B **46**, 1085 (2015)
5. M. Loidl, O. Kolk, S. Veith, T. Göbel, Materialwiss. Werkstofftech. **42**, 1105 (2011)
6. M.A. Mohtadi-Bonab, H. Ghesmati-Kucheki, Met. Mater. Int. **25**, 1109 (2019)
7. A. Drexler, C. Bergmann, G. Manke, V. Kokotin, K. Mraczek, M. Pohl, W. Ecker, Mater. Sci. Eng. A **800**, 140276 (2021)
8. S. Takagi, Y. Toji, M. Yoshino, K. Hasegawa, ISIJ Int. **52**, 316 (2012)
9. J.N. Hall, J.R. Fekete, in *Automotive Steels*, ed. by R. Rana, S.B. Singh (Woodhead Publishing, Sawston, 2017), pp. 19-45
10. M. Soleimani, H. Mirzadeh, C. Dehghanian, Met. Mater. Int. **26**, 882 (2020)
11. F. Najafkhani, H. Mirzadeh, M. Zamani, Met. Mater. Int. **25**, 1039 (2019)
12. N. Saeidi, M. Jafari, J.G. Kim, F. Ashrafizadeh, H.S. Kim, Met. Mater. Int. **26**, 168 (2020)
13. T. Senuma, ISIJ Int. **41**, 520 (2001)
14. I. Jeong, K.M. Ryu, D.G. Lee, Y. Jung, K. Lee, J.S. Lee, D.-W. Suh, Scripta Mater. **169**, 52 (2019)
15. S.K. Dwivedi, M. Vishwakarma, Int. J. Hydrogen Energy **44**, 28007 (2019)
16. B. Sun, W. Krieger, M. Rohwerder, D. Ponge, D. Raabe, Acta Mater. **183**, 313 (2020)
17. J.H. Kim, M.-H. Kwon, G. Gu, J.S. Lee, and D.-W. Suh, Materialia **12**, 100757 (2020)
18. D.K. Matlock, J.G. Speer, E. De Moor, and P.J. Gibbs, JESTECH **15**, 1 (2012)
19. J.I. Yoon, J. Jung, H.H. Lee, J.Y. Kim, H.S. Kim, Met. Mater. Int. **25**, 1161 (2019)
20. K. Rundman, R. Klug, Tran. Amer. F. **90**, 499 (1982)
21. B.D. Cullity, S.R. Stock, *Elements of X-ray Diffraction*, 3rd edn. (Prentice-Hall, Upper Saddle River, 2001), p. 351
22. ISO, 17081, Method of measurement of hydrogen permeation and determination of hydrogen uptake and transport in metals by an electrochemical technique (2004)
23. T. Narutani, Mater. Trans. JIM **30**, 33 (1989)

24. S. Oliver, T. Jones, G. Fourlaris, Mater. Charact. **58**, 390 (2007)
25. D.P. Escobar, T. Depover, L. Duprez, K. Verbeken, M. Verhaege, Acta Mater. **60**, 2593 (2012)
26. F.-G. Wei, K. Tsuzaki, Scripta Mater. **52**, 467 (2005)
27. D.P. Escobar, K. Verbeken, L. Duprez, M. Verhaege, Mater. Sci. Eng. A **551**, 50 (2012)
28. Y. Murakami, T. Kanezaki, Y. Mine, S. Matsuoka, Metall. Mater. Trans. A **39**, 1327 (2008)
29. G.R. Caskey, R.D. Sisson, Scripta Metall. **15**, 1187 (1981)
30. A. San-Martin, F.D. Manchester, Bull. Alloy Phase Diagrams **11**, 173 (1990)
31. K. Kiuchi, R.B. McLellan, Acta Metall. **31**, 961 (1983)
32. J.H. Ryu, Y.S. Chun, C.S. Lee, H. Bhadeshia, D.-W. Suh, Acta Mater. **60**, 4085 (2012)
33. Y. Park, I. Maroef, A. Landau, D. Olson, Weld. J. **81**, 27 (2002)
34. J.A. Ronevich, J.G. Speer, D.K. Matlock, SAE Int. J. Mater. Manuf. **3**, 255 (2010)
35. P. Rozenak, R. Bergman, Mater. Sci. Eng. A **437**, 366 (2006)
36. A. Laureys, T. Depover, R. Petrov, K. Verbeken, Int. J. Hydrogen Energy **40**, 16901 (2015)
37. D.-W. Suh, S.-J. Park, T.-H. Lee, C.-S. Oh, S.-J. Kim, Metall. Mater. Trans. A **41**, 397 (2010)
38. M.Y. Sherif, C.G. Mateo, T. Sourmail, H.K.D.H. Bhadeshia, Mater. Sci. Technol. **20**, 319 (2004)